

Geometrical features of wear debris

Part II *Erosion of ductile steel by liquid jet impingement*

A. W. MOMBER*[‡]

Brunnsstraße 10, D-21073 Hamburg, Germany
E-mail: andreas.momber@t-online.de

Y. C. WONG

School of Engineering and Science, Swinburne University of Technology, P.O. Box 218,
Melbourne, Victoria 3122, Australia

The erosion of metals by impinging liquid jets is a serious problem in hydraulic machines, namely pumps and turbines. Jets are formed if water or any other liquid is forced through a narrow opening, namely a pin hole, a slit, or an interface between machine parts. These openings will perform like nozzles and the liquid will be accelerated. The liquid exits the ‘nozzle’ as a liquid jet that can reach high speeds: jet speeds up to 850 m/s can be achieved for an inlet pressure of 380 MPa. Because of their high erosion capability, high-speed water jets can be used as machining tools for a wide range of materials [1]. Regarding metals, this includes sheet cutting [2], roughening [3], and profiling [4]. There are only a few studies available that deal with a detailed investigation of the processes occurring during the erosion of metals by impinging water jets, but none of them did consider morphology and size of the debris formed during the erosion process. (Micro jet and, respectively, drop impingement are not considered here; see [5] for these topics.) In this paper, the geometry of debris formed during the erosion of low-carbon steel by impinging water jets is investigated. The study may be considered in conjunction with a previous investigation, where an analysis of debris formed during solid particle impingement was performed [6].

All tests were performed with hot-rolled low-carbon steel. The steel contained the following alloying elements (given in mass%): carbon (0.13%), phosphorus (0.03%), manganese (0.50), silicon (0.03), sulphur (0.03), aluminum (0.10), titanium (0.04), micro alloys (0.01). The mechanical properties of the material were as follows: tensile strength: 350 MPa; Vickers hardness: 126 kg/mm²; yield strength: 260 MPa; grain structure: ASTM 8/100. The average grain size, estimated with a metallurgy microscope, was 25 μm. The grain structure of the material is shown in Fig. 1 of reference [6]. The specimens dimensions were 150 mm × 40 mm × 3 mm. All specimens were stored in a desiccator in order to prevent atmospheric corrosion.

The impinging liquid jet was formed in a commercial water jet cutting device that consisted of an oil-

driven pressure intensifier, a flexible pipe system, a robot-guided nozzle arrangement, and a water catcher. Two cavities, 120 mm long each, were eroded in the specimen. All erosion parameters are listed in Table I. The processes of collecting, cleaning, and analysing the wear debris are described in an accompanied paper [6]. A total number of 4400 debris was analyzed. In detail, heights (H) and widths (W) of the captured objects were measured. Hereby, H was the projection in the Y -direction, and W was the projection in the X -direction by definition. The size of the debris was defined as follows:

$$S = \frac{H + W}{2}. \quad (1)$$

The average size is given in μm. A commercial software ‘Freelancer’ was utilized to convert and calculate all image parameters. Values for the estimated parameters are listed in Table II. Scanning electron microscope (SEM) images were taken from selected samples in order to further evaluate the debris morphology.

A typical image captured by the microscope is shown in Fig. 1. Some debris are marked by circles; these samples were actually accumulations of overlapping individual debris. These samples were not considered for image analysis. Debris shape was predominantly equiaxed. The debris size histogram is displayed in Fig. 2. Two particle size parameters were used to evaluate the process, namely median diameter and mean diameter. The median diameter of the debris sample was estimated graphically from the cumulative debris diagram (see [6] for more details). The median diameter was $S_{50} = 11 \mu\text{m}$. The mean debris diameter of the debris sample is the statistical mean diameter; it was $S_0 = 15 \mu\text{m}$. Both values were about half the average grain size of the target material. Most of all debris sizes were in the range between 7.5 and 17.5 μm. The maximum size estimated in this study was about 50 μm which was about twice the average grain size of the steel.

* To whom all correspondence should be addressed.

[‡] Present address: RWTH Aachen, BGMR, Faculty of Georesources and Materials Technology, Aachen, Germany.



Figure 1 Typical image showing acquired debris.

A representative SEM-micrograph of wear debris is shown in Fig. 3a. This sample consisted of roughly equiaxed particles. Fig. 3b is an SEM-micrograph of debris taken at higher magnification. The particles showed a quasi-cleavage appearance indicating that the material was removed from a work-hardened surface. These results agreed with observations made on low-carbon steel eroded by water drops: Reference [7] noted a system of transgranular fractures which lengthened with further exposure time and gradually undermined the surface. The results from the debris size analysis agreed well with the size of the brittle features observed at the eroded surfaces. An example is shown in Fig. 4 where sizes of about $10 \mu\text{m}$ can be noted. However, 92% of all debris had sizes smaller than the target material grain size. This result agreed with results from reference [3] who found that the typical features of a surface eroded with waterjets were much smaller than

TABLE I Process parameters and erosion results

Parameter	Value
Operating pressure (MPa)	379
Jet velocity (m/s)	827
Orifice diameter (mm)	0.33
Volumetric flow rate (l/min)	3.13
Traverse rate (mm/s)	1.0
Total exposure time (s)	240
Stand-off distance (mm)	8
Eroded weight (mg)	110

TABLE II Statistical parameters of debris size analysis

Parameter	Value
Number of debris	4450
Maximum diameter	$50 \mu\text{m}$
Minimum diameter	$2 \mu\text{m}$
Mean diameter (S_0)	$14.9 \mu\text{m}$
Standard deviation	$7.8 \mu\text{m}$
Median diameter (S_{50})	$11 \mu\text{m}$

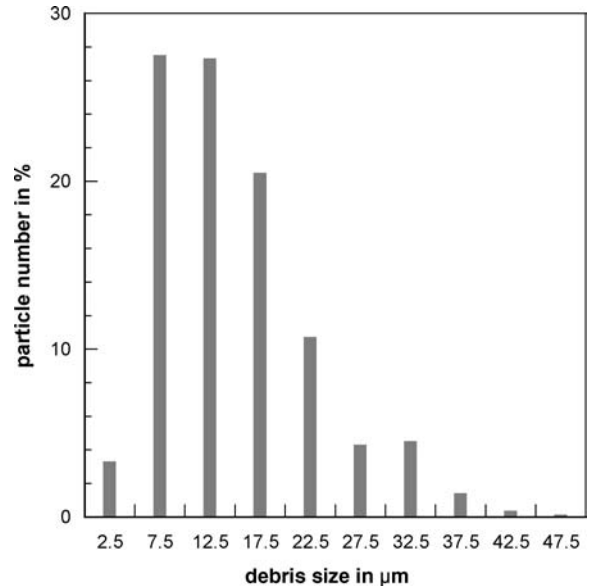


Figure 2 Wear debris size histogram.

the target material grain size. Therefore, transgranular fracture through individual grains in the material seemed to play a major role. For the stand-off distance applied in this study, a liquid jet disintegrates into individual drops; the drop size was assumed to be $3 \mu\text{m}$ for the given jet speed [8]. Therefore, the size of the brittle features and of the debris was several times larger than the drop diameter. This result pointed to a repeated high-frequency loading of the material, and Springer's [5] model may be applied to further discuss the process.

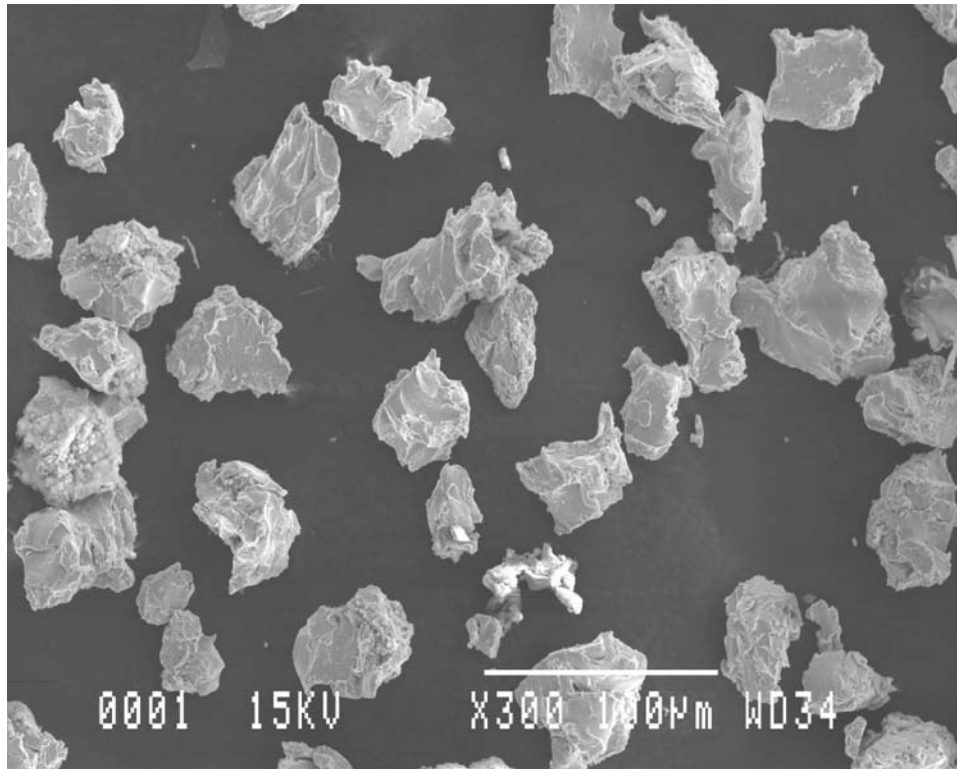
The distributions of the generated debris samples were evaluated in terms of particle size distribution functions. The standard particle size distribution functions checked in this study included the following [9]: Gaussian normal distribution; logarithmic normal distribution; Gates–Gaudin–Schumann (GGS) distribution; Rosin–Rammler–Sperling–Bennett (RRSB) distribution. The results showed that an RRSB-distribution best reflected the distribution of the debris (see Fig. 5). The coefficient of regression was 0.99. The correct equation of an RRSB-distribution is [9]:

$$\frac{f(S)}{100} = \exp \left[- \left(\frac{S}{d^*} \right)^n \right]. \quad (2)$$

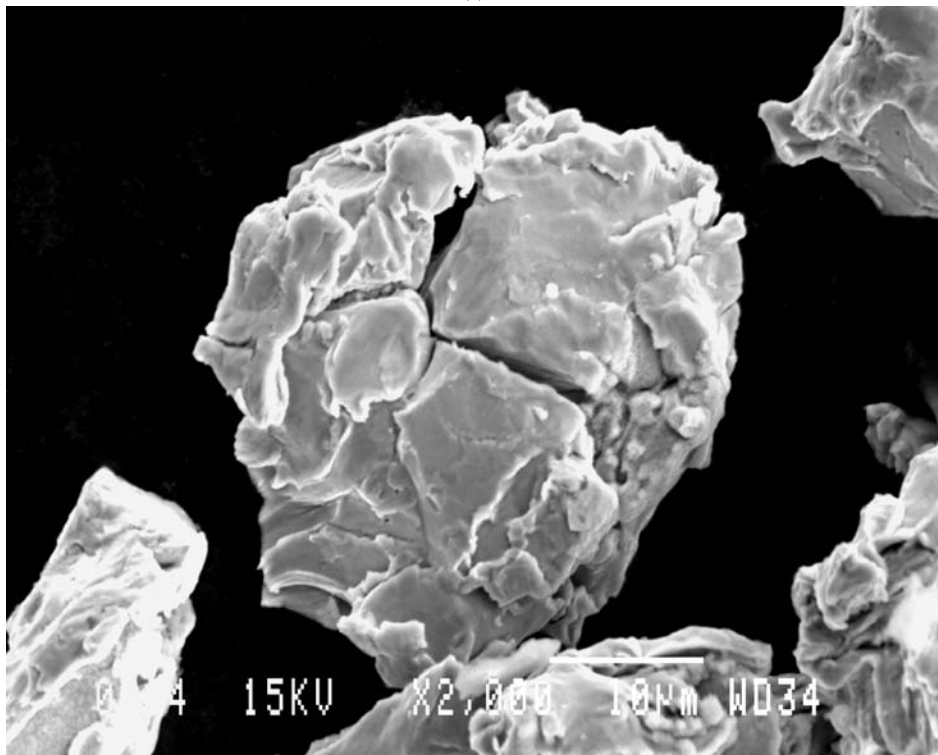
The distribution parameters d^* and n were estimated from the graph in Fig. 5; their values were $d^* = 15 \mu\text{m}$ and $n = 1.82$. The value for d^* was equal to the estimated mean debris diameter (see Table I). For comminution processes, the size parameter d^* characterizes the average distance between two activated cracks [10]. It is interesting to note that this distance was much smaller than the average grain size of the target material. Therefore, cracks did not grow along grain boundaries but rather through individual grains which is well illustrated in Fig. 4.

The results can be summarized as follows:

- Image analysis software was successfully used to analyze the geometry of wear debris.
- The statistically estimated mean debris size was about 11 μm . About 92% of all wear debris had sizes smaller than the target material grain size.
- The debris size distribution followed a Rosin–Rammler–Sperling–Bennett–distribution, whereby the distribution parameter d^* , that characterizes the average distance between activated cracks, was much smaller than the target material grain size.
- It was concluded that transgranular fracture is the major erosion mechanism in the material.



(a)



(b)

Figure 3 Wear debris formed during waterjet impingement: (a) Sample of almost spherical particles; Scale: 100 μm and (b) Higher magnification; quasi-cleavage appearance; Scale: 10 μm .

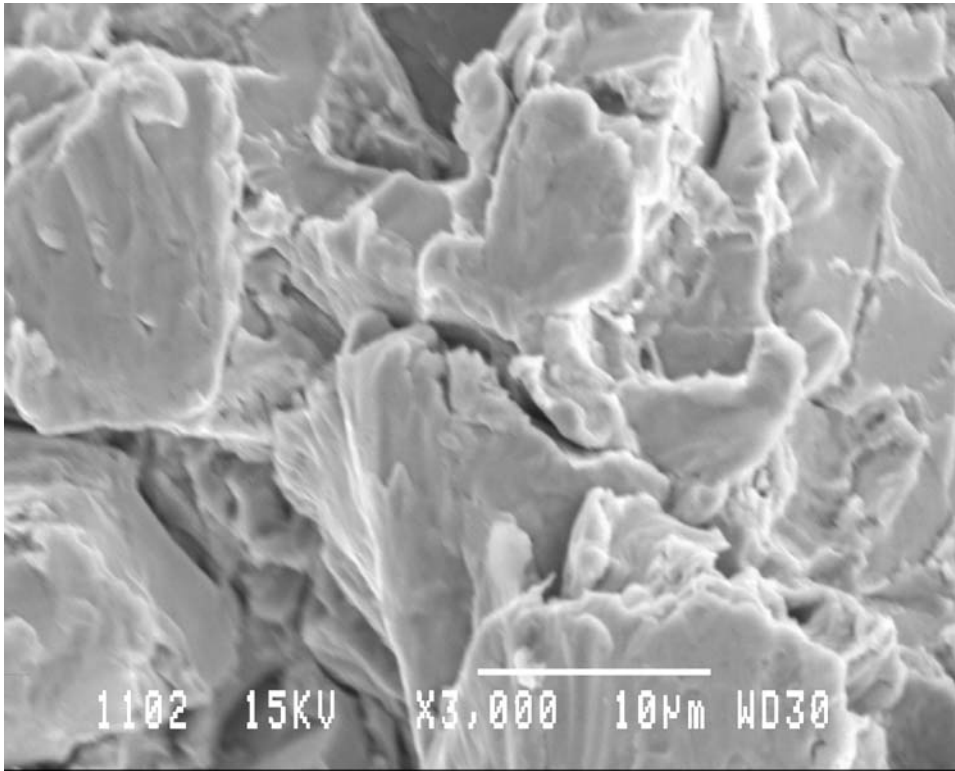


Figure 4 Brittle features at the eroded surface.

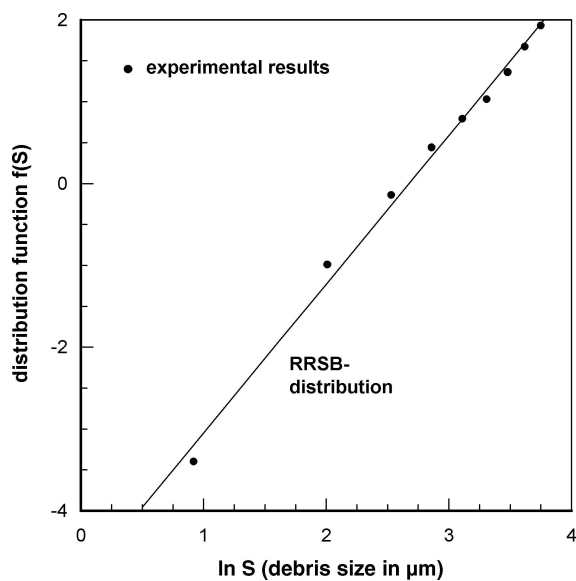


Figure 5 Rosin-Rammler-Sperling-Bennett (RRSB) distribution of the debris size.

Acknowledgments

The first author thanks the German Research Association (DFG), Bonn, Germany, for financial support.

Thanks are also addressed to IRIS, Melbourne, Australia, for technical support.

References

1. A. W. MOMBER and R. KOVACEVIC, "Principles of Abrasive Water Jet Machining" (Springer Ltd., London, 1998).
2. Sheet.
3. T. A. TAYLOR, *Surf. Coat. Technol.* **76/77** (1995) 95.
4. A. W. MOMBER, Y. WONG, E. BUDIDHARMA and R. TJO, *Wear* **249** (2002) 853.
5. G. S. SPRINGER, "Erosion by Liquid Impact" (Scripta Publishing Co., Washington D. C, 1976).
6. A. W. MOMBER and Y. C. WONG, *J. Mater. Sci.* (2004) accepted for publication.
7. N. L. HANCOX and J. H. BRUNTON, *Phil. Trans. Roy. Soc. Lond. A* **260** (1966) 121.
8. A. W. MOMBER, Y. WONG, E. BUDIDHARMA and R. TJO, *Tribol. Int.* **35** (2002) 271.
9. H. SCHUBERT, "Aufbereitung Fester mineralischer Rohstoffe," (Deutscher Verlag für Grundstoffindustrie, Leipzig, 1988) Vol. 1, p. 31.
10. J. J. GILVARRY, *J. Appl. Phys.* **32** (1961) 391.

Received 18 May
and accepted 12 August 2004